

## Accepted Manuscript

Research paper

Palladium (II) complexes based on Schiff base ligands derived from *ortho*-vanillin; synthesis, characterization and cytotoxic studies

Zeinab Faghih, Abdollah Neshat, Andrzej Wojtczak, Zahra Faghih, Zahra Mohammadi, Solmaz Varestan

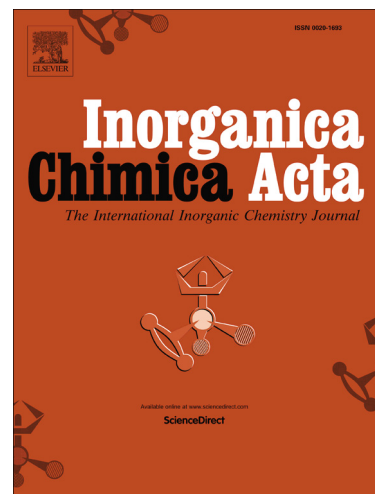
PII: S0020-1693(17)31128-3  
DOI: <https://doi.org/10.1016/j.ica.2017.11.025>  
Reference: ICA 17995

To appear in: *Inorganica Chimica Acta*

Received Date: 20 July 2017  
Revised Date: 10 November 2017  
Accepted Date: 14 November 2017

Please cite this article as: Z. Faghih, A. Neshat, A. Wojtczak, Z. Faghih, Z. Mohammadi, S. Varestan, Palladium (II) complexes based on Schiff base ligands derived from *ortho*-vanillin; synthesis, characterization and cytotoxic studies, *Inorganica Chimica Acta* (2017), doi: <https://doi.org/10.1016/j.ica.2017.11.025>

This is a PDF file of an unedited manuscript that has been accepted for publication. As a service to our customers we are providing this early version of the manuscript. The manuscript will undergo copyediting, typesetting, and review of the resulting proof before it is published in its final form. Please note that during the production process errors may be discovered which could affect the content, and all legal disclaimers that apply to the journal pertain.



# Palladium (II) complexes based on Schiff base ligands derived from *ortho*-vanillin; synthesis, characterization and cytotoxic studies

Zeinab Faghih<sup>a</sup>, Abdollah Neshat<sup>b,\*</sup>, Andrzej Wojtczak<sup>c</sup>, Zahra Faghih<sup>a</sup>, Zahra Mohammadi<sup>b</sup>, Solmaz Varestan<sup>b</sup>

<sup>a</sup> Pharmaceutical Sciences Research Center, Shiraz University of Medical Sciences, Shiraz, Iran

<sup>b</sup> Department of Chemistry, Institute for Advanced Studies in Basic Sciences (IASBS), Yousef Sobouti Blvd., Zanjan 45137-6731, Iran, [a.neshat@iasbs.ac.ir](mailto:a.neshat@iasbs.ac.ir)

<sup>c</sup> Department of Crystallochemistry and Biocrystallography, Faculty of Chemistry, Nicolaus Copernicus University in Toruń, Gagarina 7, 87-100 Toruń, Poland

## Abstract

6-Methoxy-2-[(E)-Aryliminomethyl]-phenol (Aryl = Phenyl; 2,6-dimethyl; 2,6-diisopropylphenyl; 2,6-dichlorophenyl), comprising L<sub>1</sub>-L<sub>4</sub> ligands, and palladium complexes [Pd(L<sub>n</sub>)<sub>2</sub>, n = 1-4] have been synthesized. The geometries of the [Pd(L<sub>n</sub>)<sub>2</sub>] complexes were derived from single X-ray crystallography experiments. The central Pd(II) ion is four-coordinated and surrounded by N<sub>2</sub>O<sub>2</sub> environment, adopting a square planar geometry. The ligand is bidentate, coordinating via imine nitrogen and phenolate oxygen atoms to the metal center. Analysis of the valence geometry within the phenolate rings suggests that in all complexes, the O1-C1 has a double bond character. FT-IR, <sup>1</sup>H, <sup>13</sup>C NMR and single X-ray crystal structures were reported. The cytotoxicity effect of four Pd(II) complexes was assessed on three cancerous cell lines: MCF-7 (breast carcinoma), A549 (lung carcinoma) and SKOV3 (ovarian carcinoma) and compared with that for *cis*-platin. One out of four metal complexes, Pd(L<sub>1</sub>)<sub>2</sub>, exhibited the highest anti-proliferative activity on three investigated cancerous cells lines which is more effective than *cis*-platin. The results showed that this complex could effectively induce apoptotic death in cancerous cells, probably due to direct interaction by cellular DNA.

**Key words:** Metallodrug, *cis*-platin, *ortho*-vanillin, apoptotic effect, Annexin V

## 1. Introduction

Medicinal inorganic chemistry has grown significantly in the last two decades following successes with platinum based metallodrugs in clinical tests against certain cancer cells (1-3). However, side effects of *cis*-platin has prompted search for alternative metal based drugs in fight against various types of cancers with less side effects and better cytotoxic properties compared to *cis*-platin.

Inorganic and organometallic complexes of copper [4], gold [5] and silver [6] has received particular attention in this respect. Studies show that both metal and ligand play an important role in the overall biological activity of metal based drugs. Mechanistic studies have suggested that each metal has its own unique mechanism of action against cancer cells [7,8]. The coordinated ligand also plays an important role in the anticancer activity of metallodrugs. Furthermore, ligands surrounding a metal, other than stabilizing the metal ion can modify key parameters of metal complex such as size, redox states and solubility [9-11].

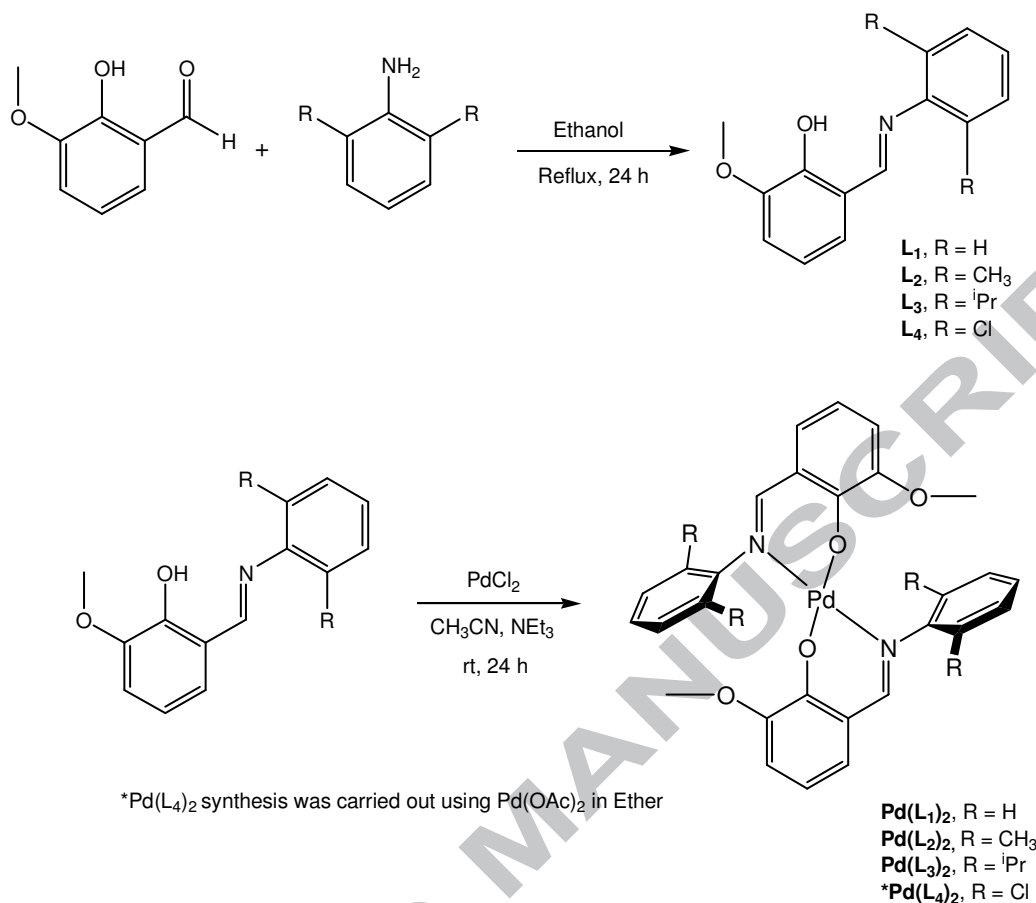
Schiff base ligands provide a great platform in coordination chemistry for the development of numerous ligand systems with controllable binding to metal ions [12-14]. Most Schiff bases are easily accessible using simple synthetic procedures and with careful selection of an amine precursor and a carbonyl compound, the nature of donor atoms and overall electronic and steric properties of Schiff bases are tunable [15-17]. Ligands in this class could potentially stabilize metals in different oxidation states and induce stability in homogeneous and heterogeneous catalysts, which is particularly useful when they are viewed in catalytic activity perspectives [18]. Metal complexes derived from Schiff bases have found applications in different research areas, including and not limited to, molecular magnetism, catalysis, and medical sciences [19-22]. Despite abundant reports regarding Schiff bases as ligands in the coordination chemistry of transition metals and their diverse applications, less research has been reported regarding palladium complexes supported with Schiff base ligands as anti-tumor agents [23-30]. In this research, the synthesis and cytotoxic properties of four palladium complexes supported with Schiff bases derived from *ortho*-vanillin have been investigated. We implemented *ortho*-vanillin in the structure of Schiff base ligands (L<sub>1</sub>-L<sub>4</sub>) because *ortho*-vanillin is a naturally occurring compound and we sought to explore biological activity of the resulting Schiff bases in combination with palladium which closely resembles platinum due to similarities of these two metals in ionic form. In order to study the effects of ligand size and electronics on the overall cytotoxicity of the palladium complexes, the ligands

L<sub>1</sub>-L<sub>4</sub> with electron donor methyl and isopropyl substituents as well as electron withdrawing chloride substituents on the phenyl ring of the imine backbone were synthesized and their cytotoxicity was tested.

## 2. Results and Discussion

### 2.1. Synthesis and characterization of palladium complexes

Synthesis of Schiff bases, L<sub>1</sub>-L<sub>4</sub>, was carried out by refluxing a solution of an aryl amine with *ortho*-vanillin in ethanol for 24 h, Scheme 1. The synthesis of Schiff base L<sub>1</sub> provided a better yield in dichloromethane solvent. Due to better solubility of palladium chloride precursor in acetonitrile and to avoid side reactions, all complexation reactions in this study were performed in this solvent by mixing and allowing to react one equivalent of palladium chloride or palladium acetate with two equivalents of corresponding Schiff bases. It is notable that Pd(L<sub>4</sub>)<sub>2</sub> complex provided higher yields in ether solution. The reactions leading to both ligand precursors and metal complexes are shown in Scheme 1. The judicious choice of aryl amine precursor allows for fine tuning of electronic and steric properties of ligands, therefore influencing the resulting metal complexes' properties. As depicted in Scheme 1, four water-soluble mononuclear Pd(II) complexes were synthesized. The ligands and metal complexes were characterized by spectroscopic methods (<sup>1</sup>H & <sup>13</sup>C NMR and IR) and in three cases the molecular structures of metal complexes were studied using single crystal X-ray crystallography.



**Scheme 1.** Synthetic route for Schiff bases (L<sub>1</sub>-L<sub>4</sub>) and corresponding Palladium complexes.

FT-IR spectrum of the free ligands, **L<sub>1</sub>-L<sub>4</sub>**, displayed a characteristic sharp bands related to aromatic and aliphatic C-H stretching vibrations between 2830 cm<sup>-1</sup> – 3100 cm<sup>-1</sup> as well as C=N and C=C and C-O stretching vibrations from 1300 cm<sup>-1</sup> to 1600 cm<sup>-1</sup>. As expected, all these bands underwent a lower or higher frequency shift after coordination of these ligands to palladium. For example, the band at ~ 1614 cm<sup>-1</sup> associated with stretching frequency of imine C=N bond in **L<sub>1</sub>** shifted to ~ 1604 cm<sup>-1</sup> in **Pd(L<sub>1</sub>)<sub>2</sub>**, indicative of imine nitrogen coordination to the metal center. Disappearance of free ligand's OH band at ~ 3200 cm<sup>-1</sup> after coordination of this functional group to metal is a strong indicative of metal complexation through anionic phenolic oxygen, however in our study this was not observed mainly due to a broad and weak OH stretching frequency bands observed in the free ligands. Therefore, a legitimate comparison of the OH vibration frequency in free and coordinated ligand was improbable.

<sup>1</sup>H NMR spectra of **L<sub>1</sub>-L<sub>4</sub>** display similar resonance patterns. <sup>1</sup>H NMR spectrum of **L<sub>2</sub>** and its palladium complex, **Pd(L<sub>2</sub>)<sub>2</sub>** are shown in Figure 1 and Figure 2., respectively. Methoxy

resonance in all free ligands was observed close to  $\delta$  4 ppm. Aromatic ring protons resonated in the range  $\delta$  6.5–7.5 ppm. Imine  $-\text{HC}=\text{N}$  resonated in the range  $\delta$  8–9 ppm in  $\text{L}_1$ – $\text{L}_3$  and at  $\delta$  10.1 ppm in  $\text{L}_4$ . Aromatic hydroxyl ( $-\text{OH}$ ) group resonated in the range  $\delta$  13–13.5 ppm in  $\text{L}_1$ – $\text{L}_3$  and an upper filed chemical shift ( $\delta$  10.6 ppm) was observed for this group in  $\text{L}_4$ .

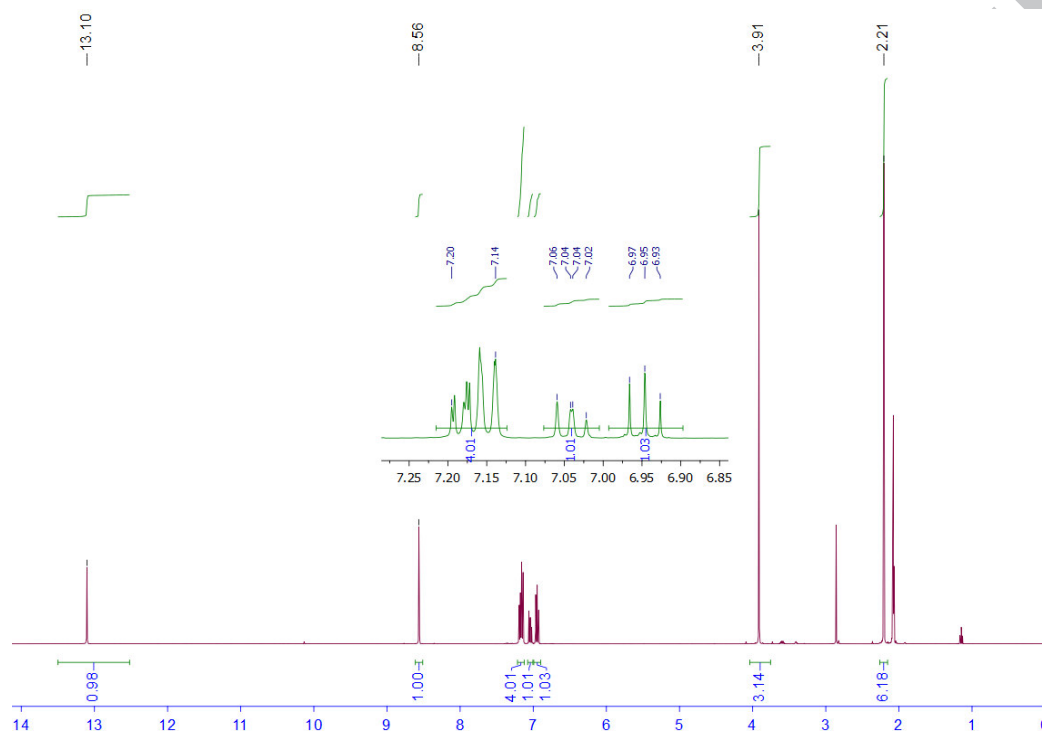


**Fig. 1.**  $^1\text{H}$  NMR spectrum of  $\text{L}_2$ . The signals from aromatic ring protons are expanded in green.

The resonances related to a hydroxyl ( $\text{OH}$ ) functional group in the free ligand is absent in metal complexes, indicating coordination of mono anionic oxygen. An upfield chemical shift was observed for the imine  $-\text{HC}=\text{N}$  moiety in all complexes compared to free ligands. This is attributable to a reduced double bond current effects in  $-\text{HC}=\text{N}$  functional group following coordination of this functional group to metal through nitrogen atom. An upfield chemical shift was also observed for methoxy resonance in palladium complexes.

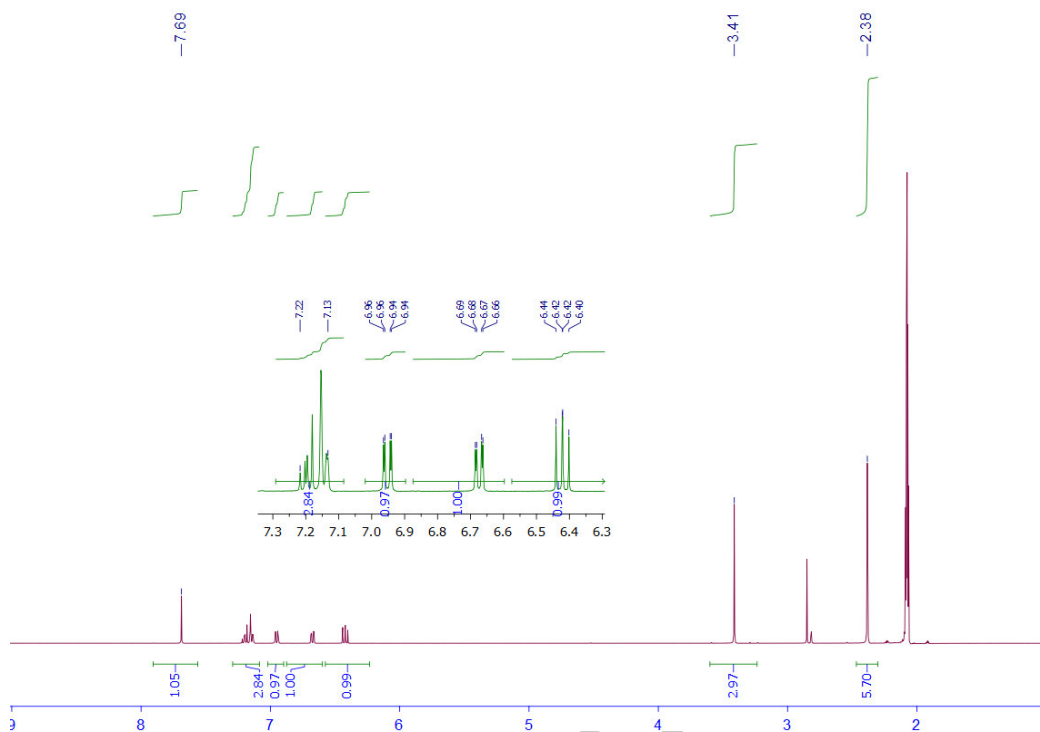


**Fig. 2.**  $^1\text{H}$  NMR spectrum of  $\text{Pd}(\text{L}_2)_2$ . The signals from aromatic ring protons are expanded in green.

The X-ray experimental data and structure refinement for the reported structures are summarized in Table 1, the selected bond lengths and angles are presented in Table S1 (ESI $^\dagger$ ). In  $\text{Pd}(\text{L}_1)_2$  and  $\text{Pd}(\text{L}_3)_2$  reported here, the complexes reveal the crystallographic  $C_i$  symmetry, with the Pd ions located on the center of symmetry. As a consequence, the asymmetric parts of these structures consist of the half of the molecule, while the other half is generated by the center of symmetry:  $[-x, -y+1, -z+1]$  for  $\text{Pd}(\text{L}_1)_2$  and  $[-x, -y, -z]$  for  $\text{Pd}(\text{L}_3)_2$ . In  $\text{Pd}(\text{L}_2)_2$  the asymmetric unit of the structure consists of the whole complex molecule. The Pd(II) coordination sphere is square-planar with the pairs of phenolate O and Schiff base N occupying the trans positions (Figs. 3–5).

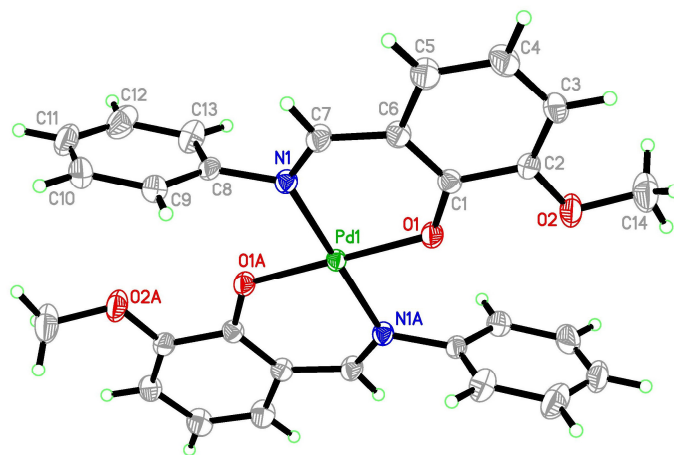


**Fig. 3.** Representations of the X-ray crystal of  $\text{Pd}(\text{L}_1)_2$  showing thermal ellipsoids for non-hydrogen atoms at 30% probability level. Selected geometrical parameters ( $\text{\AA}$ ,  $^\circ$ ): Pd1–O1A 1.9767(14), Pd1–O1 1.9768(14), Pd1–N1A 2.0179(16), Pd1–N1 2.0179(16), O1A–Pd1–O1 180.00(10), O1A–Pd1–N1A 91.66(6), O1–Pd1–N1A 88.34(6), O1A–Pd1–N1 88.34(6), O1–Pd1–N1 91.66(6), N1–Pd1–N1A 180.0.

In the reported complexes, the Pd–O bonds formed by the phenolate atoms range from 1.964(4) to 1.980(4)  $\text{\AA}$ , both found in  $\text{Pd}(\text{L}_3)_2$ , and are significantly shorter than the Pd–N distances varying from 2.008(5) to 2.0179(16)  $\text{\AA}$  (Table S1 in ESI<sup>†</sup>). The N–Pd–O angles involving atoms of the same ligand are larger by approximately 4–5 $^\circ$  than those involving atoms of different ligands. That observation might be related to the rigidity of the ligand. In fact, the exocyclic O1–C1–C6 and C1–C6–C7 angles of almost 126 $^\circ$  and 123 $^\circ$ , respectively, are significantly larger than their counterparts O1–C1–C2 and C5–C6–C7 angles being both approximately 117 $^\circ$ .

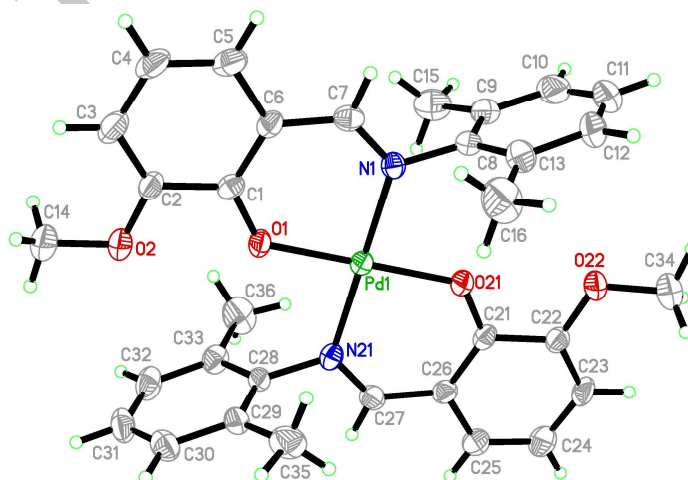


**Fig. 4.** Thermal ellipsoids for non-hydrogen atoms are plotted at 30% probability level. Selected geometrical parameters ( $\text{\AA}$ ,  $^\circ$ ): Pd1–O1 1.964(4), Pd1–O21 1.980(4), Pd1–N21 2.008(5), Pd1–N1 2.017(5), O1–Pd1–O21 179.6(2), O21–Pd1–N21 92.54(19), O1–Pd1–N21 87.19(19), O21–Pd1–N1 87.73(19), O1–Pd1–N1 92.54(19), N21–Pd1–N1 179.3(2).

In all complexes the ligand is a phenolate monoanion. However, analysis of the valence geometry within the phenolate rings suggests that in all complexes, the O1–C1 has a double bond character, with the O–C distances ranging from 1.299(7) Å in **Pd(L<sub>2</sub>)<sub>2</sub>** to 1.307(2) Å in **Pd(L<sub>1</sub>)<sub>2</sub>**. Furthermore, the average distances of the C2–C3 and C4–C5 bonds, being 1.364 and 1.352 Å (Table 2), are significantly shorter than other intra-ring distances that range from 1.392(10) to 1.443(9) Å. These experimental data suggests that the ligands exist in the quinone form. Also the methoxy substituents at C2 position reveal C2–O2 bond distances of 1.356(8) Å in **Pd(L<sub>2</sub>)<sub>2</sub>** to 1.374(4) Å in **Pd(L<sub>3</sub>)<sub>2</sub>**.

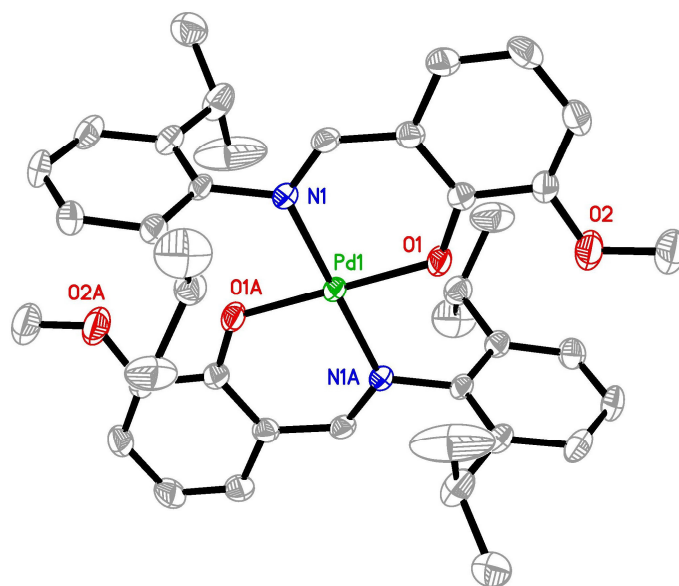


**Fig. 5.** Representations of the X-ray crystal of **Pd(L<sub>3</sub>)<sub>2</sub>** with thermal plotted at 30% probability level. Hydrogen atoms are omitted for clarity. Selected geometrical parameters (Å, °): Pd1–O1A 1.972(2), Pd1–O1 1.972(2), Pd1–N1A 2.017(2), Pd1–N1 2.017(2), O1A–Pd1–O1 180.00(11), O1A–Pd1–N1A 92.28(10), O1–Pd1–N1A 87.72(10), O1A–Pd1–N1 87.72(10), O1–Pd1–N1 92.28(10), N1A–Pd1–N1 180.0.

In all complexes, the methoxy group is rotated away from the phenolate O1, with the absolute value of the torsion angles C1–C2–O2–C14 ranging from 166.4(6) in **Pd(L<sub>2</sub>)<sub>2</sub>** to 173.6(4)° in **Pd(L<sub>3</sub>)<sub>2</sub>**.

Furthermore, the Schiff base moiety is co-planar with the phenolate ring, with the torsion angles C1–C6–C7–N1 ranging from –3.6(6) in **Pd(L<sub>3</sub>)<sub>2</sub>** to 0.0(4)° in **Pd(L<sub>1</sub>)<sub>2</sub>**. The resulting conformation of the six-membered chelate ring is flat, with the average absolute values of torsion angles being 4.3, 5.7/4.5 and 3.5° for **Pd(L<sub>1</sub>)<sub>2</sub>**, two rings in **Pd(L<sub>2</sub>)<sub>2</sub>** and in **Pd(L<sub>3</sub>)<sub>2</sub>**, respectively. The significant twist is detected around N1–C8 bond of each ligand, that results in almost perpendicular orientation of the phenolic and phenyl rings, with dihedral angles

between their best planes being 75.99(12), 84.0(4)/89.5(4) and 78.03(19)° for **Pd(L<sub>1</sub>)<sub>2</sub>**, **Pd(L<sub>2</sub>)<sub>2</sub>** and **Pd(L<sub>3</sub>)<sub>2</sub>**, respectively.

**Table 1.** Crystal data and structure refinement for **Pd(L<sub>1</sub>)<sub>2</sub>**, **Pd(L<sub>2</sub>)<sub>2</sub>** and **Pd(L<sub>3</sub>)<sub>2</sub>**

Identification code	<b>Pd(L<sub>1</sub>)<sub>2</sub></b>	<b>Pd(L<sub>2</sub>)<sub>2</sub></b>	<b>Pd(L<sub>3</sub>)<sub>2</sub></b>
Empirical formula	C <sub>28</sub> H <sub>24</sub> N <sub>2</sub> O <sub>4</sub> Pd	C <sub>32</sub> H <sub>32</sub> N <sub>2</sub> O <sub>4</sub> Pd	C <sub>40</sub> H <sub>48</sub> N <sub>2</sub> O <sub>4</sub> Pd
Formula weight	558.89	614.99	727.20
Temperature; K	293(2)	293(2)	293(2)
Wavelength; Å	0.71073	0.71073	0.71073
Crystal system	Orthorhombic	Orthorhombic	Triclinic
Space group	Pbca	P2 <sub>1</sub> 2 <sub>1</sub> 2 <sub>1</sub>	P-1
Unit cell dimensions; Å, °	a = 14.7061(11)	a = 8.2157(7)	a = 9.0269(8)
	b = 10.2942(8)	b = 17.6417(17)	b = 10.1666(9)
	c = 16.4768(13)	c = 19.903(2)	c = 10.7579(9)
	α = 90	α = 90	α = 69.924(8).
	β = 90	β = 90	β = 89.144(7)
	γ = 90	γ = 90	γ = 85.639(8)
Volume; Å <sup>3</sup>	2494.4(3)	2884.7(5)	924.55(15)
Z	4	4	1
Density (calculated); Mg/m <sup>3</sup>	1.488	1.416	1.306
Absorption coefficient; mm <sup>-1</sup>	0.780	0.682	0.543
F(000)	1136	1264	380
Crystal size; mm	0.559 x 0.411 x 0.137	0.612 x 0.276 x 0.081	0.632 x 0.395 x 0.167
Theta range for data collection	2.472 to 28.503°.	2.309 to 28.587°.	2.139 to 28.432°.
Index ranges	-15 ≤ h ≤ 18, -8 ≤ k ≤ 13, -21 ≤ l ≤ 21	-10 ≤ h ≤ 10, -23 ≤ k ≤ 21, -26 ≤ l ≤ 24	-11 ≤ h ≤ 7, -13 ≤ k ≤ 13, -13 ≤ l ≤ 13

Reflections collected	16520	20234	6389
Independent reflections	2952 [R(int) = 0.0361]	6662 [R(int) = 0.0666]	4111 [R(int) = 0.0586]
Completeness to theta	25.242° 100.0 %	25.242° 99.9 %	25.242° 99.9 %
Absorption correction	Analytical	Analytical	Analytical
Max. and min. transmission	0.974 and 0.909	0.955 and 0.725	0.971 and 0.904
Refinement method	Full-matrix least-squares on F <sup>2</sup>	Full-matrix least-squares on F <sup>2</sup>	Full-matrix least-squares on F <sup>2</sup>
Data / restraints / parameters	2952 / 0 / 160	6662 / 0 / 352	4111 / 0 / 214
Goodness-of-fit on F <sup>2</sup>	1.047	1.051	1.109
Final R indices [I>2sigma(I)]	R1 = 0.0277, wR2 = 0.0589	R1 = 0.0520, wR2 = 0.0875	R1 = 0.0533, wR2 = 0.1147
R indices (all data)	R1 = 0.0473, wR2 = 0.0682	R1 = 0.0886, wR2 = 0.0981	R1 = 0.0619, wR2 = 0.1232
Flack x	n/a	-0.04(2)	n/a
Largest diff. peak and hole; e.Å <sup>-3</sup>	0.304 and -0.454	1.131 and -1.026	0.660 and -0.702

## 2.2 Cytotoxic Effects of Pd(II) Complexes

The cytotoxicity effects of four Pd(II) complexes were assessed on three cancerous cell lines: MCF-7 (breast carcinoma), A549 (lung carcinoma) and SKOV3 (ovarian carcinoma). As shown in Table 2, among four compounds, **Pd(L<sub>1</sub>)<sub>2</sub>** demonstrated the best cytotoxic effect on almost all three cell lines with IC<sub>50</sub> of 7.21 ± 1.71, 14.72 ± 5.82 and 21.79 ± 3.07 on MCF-7, A549 and SKOV3, respectively. This complex also appeared to be more effective than *cis*-platin (, 61.56 ± 0.98, 50.81 ± 3.10 and 43.81 ± 3.79, respectively). **Pd(L<sub>2</sub>)<sub>2</sub>** and **Pd(L<sub>4</sub>)<sub>2</sub>** have shown weak cytotoxic effects on three investigated cell lines (IC<sub>50</sub>>100).

**Table 2.** In vitro cytotoxicity effect of Pd(II) complexes on cancer cell lines

Pd(II) Complex	IC <sub>50</sub>		
	MCF-7	A549	SKOV3
Pd(L <sub>1</sub> ) <sub>2</sub>	7.21 ± 1.71	14.72 ± 5.82	21.79 ± 3.07
Pd(L <sub>2</sub> ) <sub>2</sub>	>100	>100	>100
Pd(L <sub>3</sub> ) <sub>2</sub>	89.21 ± 3.22	>100	>100
Pd(L <sub>4</sub> ) <sub>2</sub>	>100	>100	>100
<i>cis-platin</i>	61.56 ± 0.98	50.81 ± 3.10	43.81 ± 3.79

\* IC<sub>50</sub>: Inhibitory concentration 50

### 2.3 Apoptosis Assay

In the next step, we assessed the capacity of Pd(L<sub>1</sub>)<sub>2</sub> in the induction of apoptosis in MCF-7 cell line by Annexin V/7AAD kit, which is specifically designed for detecting apoptotic and necrotic cells. Annexin V binds to phosphatidylserine (PS) which is normally found on the intracellular membrane in live intact cells. During apoptosis, in the early step, the asymmetry of membrane is lost and PS is transferred to the external layer. To distinguish necrotic cells from apoptotic cells, 7AAD was also used; as early apoptotic cells will exclude 7AAD, whereas the apoptotic cells in the late stage as well as necrotic cells absorb 7AAD, which in turn goes into the nucleus and binds to DNA. As it is observed in Figure 6, Pd(L<sub>1</sub>)<sub>2</sub> could effectively induce more apoptosis along with an increase in its concentration (early apoptosis increased from 5.32% at 2 μM to 41.5% at 14 μM).

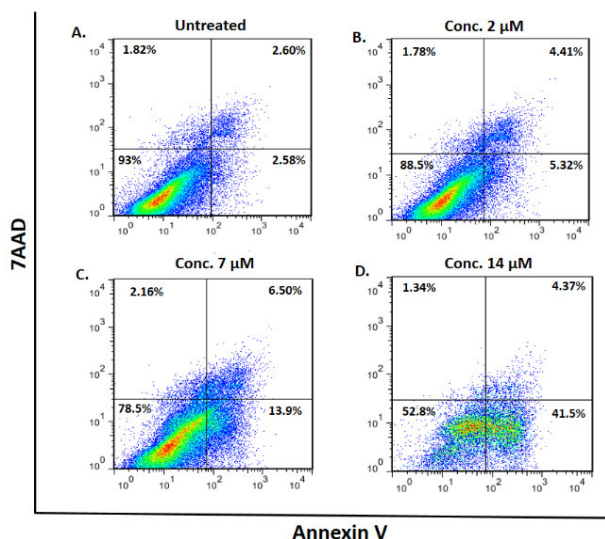


**Fig. 6.** Determination of apoptotic effect of  $\text{Pd}(\text{L}_1)_2$  on MCF-7 cell line. 7AAD stains dead cells. Increased levels of Annexin V+ apoptotic cells in treated cells comparing to untreated cells is an indicative that  $\text{Pd}(\text{L}_1)_2$  can inhibit tumor cells' growth through induction of apoptosis. Early apoptosis: 7AAD/Annexin V<sup>+</sup>; late apoptosis: 7AAD<sup>+</sup>/Annexin V<sup>+</sup>; necrosis: 7AAD<sup>+</sup>/Annexin V<sup>-</sup>; viable cells: 7AAD/Annexin V<sup>-</sup>

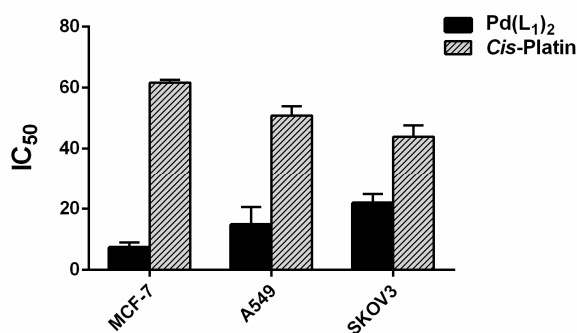


**Fig. 7.** Significantly higher in vitro cytotoxicity of  $\text{Pd}(\text{L}_1)_2$  on MCF-7, A549 and SKOV3 cell lines in comparison to *cis*-platin

## 2.4 Solution Stability Studies

The stability of palladium complexes  $\text{Pd}(\text{L}_1)_2$ ,  $\text{Pd}(\text{L}_2)_2$  and  $\text{Pd}(\text{L}_3)_2$  in the aqueous biological media was evaluated by monitoring the <sup>1</sup>H NMR spectra of these compounds (1 mM) in 50 mM phosphate buffer over a period of 10 days. Few drops of acetone-*d*<sub>6</sub> were added to solubilize the compound in the aqueous media. The obtained spectra are shown in the Supporting information (Figures S1-S3). In all three compounds, the first spectrum was recorded after 5 minutes of mixing and shaking solute with NMR solvent. Then, the rest of

the spectra were recorded with 24 h time gap. No obvious sign of degradation is observed in the  $^1\text{H}$  NMR spectra of all three complexes even after 10 days. It is notable that the quality of signals in the aqueous media is lower than that of pure deuterated acetone.

## 2.5 Interaction of $\text{Pd}(\text{L}_1)_2$ with DNA

Many chemotherapeutic drugs particularly metal-based drugs target DNA replication, a crucial event in cell division which is overactive in tumor cells. Most of these compounds act through binding to DNA and these interaction leads a shift in the mobility of DNA. We used electrophoresis mobility shift assay to evaluate the interaction of  $\text{Pd}(\text{L}_1)_2$  with DNA. As demonstrated in Figure 8, both *cis*-platin, as positive control, (A) and  $\text{Pd}(\text{L}_1)_2$  (B) make an obvious shift in the mobility of the plasmid in comparison to untreated DNA showing their interactions with DNA. These results suggested that at least a part of cytotoxic effects of  $\text{Pd}(\text{L}_1)_2$ , is exerted through its direct interaction with DNA.

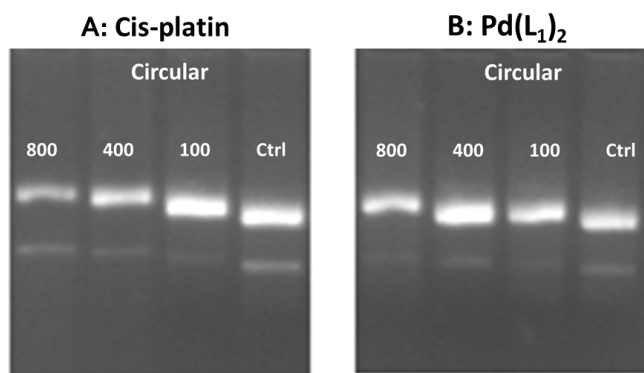


**Fig. 8.** Electrophoresis mobility shift assay for  $\text{Pd}(\text{L}_1)_2$ . pET28a plasmid in circular format was incubated with different concentrations of *cis*-platin (A) and  $\text{Pd}(\text{L}_1)_2$  (B).

## 3. Conclusion

As demonstrated in Figure 7 and Table 2, among palladium complexes reported in this study,  $\text{Pd}(\text{L}_1)_2$  exhibited the highest anti-proliferative activity on three investigated cancerous cells lines which is even higher than *cis*-platin. It is quite clear that the cytotoxicity activity of these complexes are highly dependent on the nature of the substituents present on the phenyl ring. Single X-ray crystallography results reveal that the nature of the substituents does not affect the geometry of the complex and all complexes adopt a square planar geometry with no

distortion around metal center. An unsubstituted phenyl ring in *ortho* positions such as the one in  $\text{Pd}(\text{L}_1)_2$  has a reduced steric hindrance compared to other complexes in this study and this might affect dissociation pattern of the ligand from metal center inside the cell, influencing overall cytotoxic activity of this complex. The data obtained from apoptosis study also confirmed the cytotoxic studies, as  $\text{Pd}(\text{L}_1)_2$  effectively activates apoptosis pathway in cancer cells. This result is consistent with some recent studies showing that Pd(II) complexes could induce apoptosis in tumor cells [30, 31]. As represented shift assay results indicated, similar to *cis*-platin,  $\text{Pd}(\text{L}_1)_2$  could directly bind to cellular DNA. It implies that, at least in part,  $\text{Pd}(\text{L}_1)_2$  cytotoxic effect is probably mediated through interaction with DNA as *cis*-platin does. Overall, initial results represented in this study indicated that the new Pd(II) complex,  $\text{Pd}(\text{L}_1)_2$ , can be introduced as a novel potential drug in treating cancer in particular breast carcinoma. However, through which mechanisms this compound inhibits proliferation or function of cancerous cells and/or the effect of this compound on other cancerous cells remains to be elucidated.

## 4. Experimental

### 4.1. General Procedures and Materials

Reagents and solvents were used as received from commercial suppliers.  $^1\text{H}$ ,  $^{13}\text{C}\{^1\text{H}\}$  NMR spectra were recorded on a Bruker Avance DPX 400 MHz instrument in Acetone- $d_6$  at 25 °C using standard pulse programs.  $^1\text{H}$  and  $^{13}\text{C}$  shifts are quoted relative to the residual solvent signals. Infrared spectra were measured on a Bruker Vertex 70 FT-IR spectrometer.

### 4.2 Synthesis of Ligands and Palladium Complexes

#### 4.2.1. Synthesis of $\text{L}_1$ , 6-Methoxy-2-[(E)-phenyliminomethyl]-phenol

*Ortho*-vanillin (0.50 g, 3.3 mmol) was added to a solution of aniline (0.3 g, 3.3 mmol) in ethanol. The mixture was refluxed for 24 h. The orange precipitate was removed by filtration and washed with n-hexane. Re-crystallization from ethanol solution (20 mL) at 0 °C yielded analytically pure orange crystals. Yield: 0.645 g, 86%. Mp: 86 °C.  $^1\text{H}$  NMR (Acetone- $d_6$ , 400 MHz):  $\delta$  13.38 (s, 1H), 8.9 (s, 1H, Ar H), 7.510-7.419 (m, 4H, Ar H), 7.338 (t, 1H,  $J = 8.0$  Hz, Ar H), 7.214 (dd, 1H,  $J = 8.0$  Hz,  $^4J = 4.0$  Hz, Ar H), 7.132 (dd, 1H,  $J = 8.0$  Hz,  $^4J = 4.0$  Hz, Ar H), 6.927 (t, 1H,  $J = 8.0$  Hz, Ar H), 3.893 (s, 3H).  $^{13}\text{C}\{^1\text{H}\}$  NMR (Acetone- $d_6$ , 100 MHz)  $\delta$  163.88, 151.64, 148.58, 148.45, 129.47, 126.95, 124.31, 121.29, 119.42, 118.52, 115.73, 55.64. IR: 3100 (w), 2985 (w), 2972 (w), 2197 (w), 1995 (w), 1900 (w), 1880 (w), 1770 (w), 1720 (w), 1614 (s), 1585 (s), 1486 (m), 1466 (s), 1409 (m), 1363 (m), 1329 (w),

1266 (s), 1253 (s), 1195 (s), 1169 (w), 1075 (s), 1000 (w), 995 (s), 920 (w), 856 (w), 831 (w), 811 (s), 782 (s), 766 (s), 734 (s), 690 (s), 590 (w), 495 (w), 380 (w).

#### 4.2.2 Synthesis of **L<sub>2</sub>**, 6-Methoxy-2-[(E)-2,6-dimethylphenyliminomethyl]-phenol

*Ortho*-vanillin (1.0 g, 6.6 mmol) was added to a solution of 2,6-dimethylaniline (0.8 g, 6.6 mmol) in ethanol. The mixture was refluxed for 20 h. The orange precipitate was collected upon concentration of ethanol solution and removed by filtration and washed with n-hexane. Re-crystallization from acetone solution (20 mL) at room temperature yielded analytically pure orange crystals. Yield: 1.47 g, 88%. Mp: 143 °C. <sup>1</sup>H NMR (Acetone-*d*<sub>6</sub>, 400 MHz): δ 13.103 (s, 1H), 8.564 (s, 1H, Ar H), 7.20-7.140 (m, 4H, Ar H), 7.040 (t, 1H, *J* = 8.0 Hz, Ar H), 6.946 (t, 1H, *J* = 8.0 Hz, Ar H), 3.914 (s, 3H), 2.205 (s, 6H). <sup>13</sup>C NMR (Acetone-*d*<sub>6</sub>, 100 MHz) δ 168.13, 151.59, 148.62, 148.29, 128.31, 128.04, 124.90, 124.09, 119.01, 118.50, 115.71, 55.58, 17.64. IR: 3450 (br.), 2955 (w), 2931 (w), 1623 (s), 1590 (w), 1465 (s), 1416 (w), 1365 (w), 1330 (w), 1270 (m), 1249 (s), 1185 (s), 1090 (w), 1075 (w), 966 (m), 852 (w), 839 (w), 786 (w), 769 (m), 742 (w), 718 (w).

#### 4.2.3. Synthesis of **L<sub>3</sub>**, 6-Methoxy-2-[(E)-2,6-diisopropylphenyliminomethyl]-phenol

*Ortho*-vanillin (1.0 g, 6.6 mmol) was added to a solution of 2,6-diisopropylaniline (1.17 g, 6.6 mmol) in ethanol. The mixture was refluxed for 20 h. The orange colored precipitate was formed upon concentration. The red solid was washed with n-hexane solution (2 × 10 mL) and was collected by filtration. Re-crystallization from ethanol solution (20 mL) at 0 °C yielded analytically pure orange crystals. Yield: 1.78 g, 87%. Mp: 148 °C. <sup>1</sup>H NMR (Acetone-*d*<sub>6</sub>, 400 MHz): δ 13.074 (s, 1H), 8.544 (s, 1H, Ar H), 7.263-7.173 (m, 5H, Ar H), 6.961 (t, 1H, *J* = 8.0 Hz, Ar H), 3.921 (s, 3H), 3.036 (sept, 2H, *J* = 7.2 Hz), 1.198 (d, 12H, *J* = 7.2 Hz). <sup>13</sup>C{<sup>1</sup>H} NMR (Acetone-*d*<sub>6</sub>, 100 MHz) δ 168.01, 151.54, 148.66, 146.38, 138.42, 125.48, 124.05, 123.18, 118.90, 118.64, 115.75, 55.56, 28.01, 22.85. IR: 3040 (w), 2962 (s), 2925 (m), 2899 (m), 2866 (m), 1620 (s), 1584 (m), 1457 (s), 1408 (m), 1362 (m), 1326 (m), 1254 (s), 1179 (s), 1096 (m), 1074 (m), 967 (s), 910 (w), 855 (m), 832 (m), 780 (m), 762 (m), 737(m).

#### 4.2.4 Synthesis of **L<sub>4</sub>**, 6-Methoxy-2-[(E)-2,6-dichlorophenyliminomethyl]-phenol

*Ortho*-vanillin (0.5 g, 3.3 mmol) was added to a solution of 2,6-dichloroaniline (0.53 g, 3.3 mmol) in ethanol. The mixture was refluxed for 20 h. Then, solvent was removed under vacuum. Viscous yellow liquid was analyzed using thin layer chromatography (3:1, dichloromethane : n-hexane solvents) and it showed, other than desired product, a side

product and minor unreacted *Ortho*-vanillin. Attempts to solidify this viscous liquid in polar and non-polar solvents were not successful. Pure product was obtained using plate chromatography in 3:1 ratio of dichloromethane and n-hexane solvents. Yield: 0.7 g, 72%.  $^1\text{H}$  NMR (Acetone- $d_6$ , 400 MHz):  $\delta$  10.61 (br. s, 1H), 10.12 (s, 1H, Ar H), 7.34 (dd, 1H,  $J = 8.0$  Hz,  $^4J = 1.6$  Hz, Ar H), 7.28 (dd, 1H,  $J = 8.0$  Hz,  $^4J = 1.6$  Hz, Ar H), 7.24 (d, 2H,  $J = 8.0$  Hz, Ar H), 7.00 (t, 1H,  $J = 8.0$  Hz, Ar H), 6.65 (t, 1H,  $J = 8.0$  Hz, Ar H), 3.90 (s, 3H).  $^{13}\text{C}\{^1\text{H}\}$  NMR (Acetone- $d_6$ , 100 MHz)  $\delta$  195.98, 151.55, 148.36, 128.83, 127.96, 123.58, 121.43, 119.50, 118.89, 118.14, 117.44, 55.72. IR: 3589 (w), 3568 (w), 3547 (w), 3525 (w), 3482 (w), 3453 (w), 3385 (w), 2980 (w), 2965 (w), 2750 (w), 1654 (m), 1619 (m), 1464 (s), 1390 (w), 1325 (w), 1256 (s), 1218 (w), 1073 (w), 954 (w), 777 (w), 764 (w), 737 (w), 720 (w).

#### 4.2.5. Synthesis of Pd(L<sub>1</sub>)<sub>2</sub>

In a flask, L<sub>1</sub> (0.102 g, 0.44 mmol) was dissolved in 10 mL dichloromethane and PdCl<sub>2</sub> (0.04 g, 0.22 mmol) was also added to the flask. Triethylamine (NEt<sub>3</sub>, 0.045 g, 0.44 mmol) was added as base. The mixture stirred at room temperature for 24 h. Then, red precipitate was collected by filtration and it was washed with n-hexane to remove remaining L<sub>1</sub>. Recrystallization of red precipitate from acetone solution resulted in orange crystals suitable for X-ray diffraction analyses. Yield: 0.066 g, 52%. Mp: 249 °C.  $^1\text{H}$  NMR (Acetone- $d_6$ , 400 MHz):  $\delta$  7.91 (s, 2H, Ar H), 7.43-7.39 (m, 10H, Ar H), 6.99 (dd, 2H,  $J = 8.0$  Hz,  $^4J = 4.0$  Hz, Ar H), 6.68 (dd, 2H,  $J = 8.0$  Hz,  $^4J = 4.0$  Hz, Ar H), 6.44 (d, 2H,  $J = 8.0$  Hz, Ar H), 3.34 (s, 6H).  $^{13}\text{C}\{^1\text{H}\}$  NMR (Acetone- $d_6$ , 100 MHz):  $\delta$  163.67, 150.97, 150.06, 128.20, 126.23, 125.90, 124.86, 121.27, 119.95, 115.30, 113.98, 45.45. IR: 3441 (br.), 3081 (w), 3052 (w), 3004 (w), 2950 (w), 2924 (w), 2829 (w), 1604 (s), 1590 (s), 1541 (s), 1448 (m), 1462 (s), 1441 (s), 1386 (w), 1356 (w), 1326 (s), 1240 (s), 1186 (s), 1110 (m), 1077 (m), 1025 (w), 1001 (w), 988 (m), 970 (w), 911 (w), 882 (w), 857 (w), 781 (w), 739 (m), 694 (s), 591 (w), 552 (m).

#### 4.2.6. Synthesis of Pd(L<sub>2</sub>)<sub>2</sub>

In a flask, L<sub>2</sub> (0.15 g, 0.59 mmol) was dissolved in 10 mL acetonitrile and PdCl<sub>2</sub> (0.052 g, 0.30 mmol) was added to the flask. Triethylamine (NEt<sub>3</sub>, 0.06 g, 0.59 mmol) was added as base. The mixture stirred at room temperature for 24 h. Then, red precipitate was collected by filtration and it was washed with n-hexane to remove any remaining L<sub>2</sub>. Recrystallization of red precipitate from acetone solution resulted in orange crystals suitable for X-ray diffraction analyses. Yield: 0.06 g, 33%. Mp: 308 °C.  $^1\text{H}$  NMR (Acetone- $d_6$ , 400 MHz):  $\delta$  7.69 (s, 2H,

Ar H), 7.22-7.13 (m, 6H, Ar H), 6.95 (dd, 2H,  $J = 8.0$  Hz,  $^4J = 4.0$  Hz, Ar H), 6.67 (dd, 2H,  $J = 8.0$  Hz,  $^4J = 4.0$  Hz, Ar H), 6.42 (t, 2H,  $J = 8.0$  Hz, Ar H), 3.41 (s, 6H), 2.383 (s, 6H).  $^{13}\text{C}\{^1\text{H}\}$  NMR (Acetone- $d_6$ , 100 MHz):  $\delta$  164.07, 156.96, 151.07, 148.06, 131.71, 127.82, 125.84, 125.58, 120.24, 114.58, 113.70, 54.65, 18.38. IR: 3500 (br.), 2975 (m), 2937 (m), 2758 (w), 2738 (w), 2676 (m), 2622 (m), 2603 (m), 2500 (w), 2495 (m), 1605 (s), 1538 (w), 1468 (s), 1439 (s), 1397 (w), 1328 (m), 1253 (s), 1233 (w), 1157 (m), 1029 (w), 1035 (w), 986 (w), 856 (w), 734 (w).

#### 4.2.7. Synthesis of Pd(L<sub>3</sub>)<sub>2</sub>

In a flask, L<sub>3</sub> (0.088 g, 0.28 mmol) was dissolved in 10 mL acetonitrile and PdCl<sub>2</sub> (0.025 g, 0.14 mmol) was also added to the flask. Triethylamine (NEt<sub>3</sub>, 0.029 g, 0.28 mmol) was added as base. The mixture stirred at room temperature for 48 h. Then, red precipitate was collected by filtration and it was washed with n-hexane to remove any remaining L<sub>3</sub>. Due to solubility of the metal complex, Pd(L<sub>3</sub>)<sub>2</sub>, in acetonitrile, the red colored supernatant was left in ambient temperature to slowly evaporate and to solidify. The collected solid was dissolved in acetone to remove any remaining trimethylamine hydrochloride salt. Finally, red solution in acetone was slowly evaporated to yield suitable crystals for X-ray analysis. Yield: 0.07 g, 69%. Mp: 284 °C.  $^1\text{H}$  NMR (Acetone- $d_6$ , 400 MHz):  $\delta$  7.75 (s, 2H, Ar H), 7.37 (t, 3H,  $J = 8.0$  Hz, Ar H), 7.25 (d, 4H,  $J = 8.0$  Hz, Ar H), 6.99 (dd, 2H,  $J = 8.0$  Hz,  $^4J = 4.0$  Hz, Ar H), 6.68 (dd, 2H,  $J = 8.0$  Hz,  $^4J = 4.0$  Hz), 6.41 (t, 2H,  $J = 8.0$  Hz), 3.67 (sept, 4H,  $J = 7.2$  Hz), 3.29 (s, 6H), 1.33 (d, 12H,  $J = 7.2$  Hz), 1.19 (d, 12H,  $J = 7.2$  Hz).  $^{13}\text{C}\{^1\text{H}\}$  NMR (Acetone- $d_6$ , 100 MHz):  $\delta$  168.01, 151.54, 148.66, 146.38, 138.42, 125.48, 124.05, 123.18, 118.90, 118.64, 115.75, 55.56, 28.01, 22.85. IR: 3085 (w), 2959 (w), 2924 (w), 2866 (w), 1603 (s), 1540 (w), 1464 (m), 1437 (m), 1382 (w), 1362 (w), 1326 (m), 1244 (m), 1220 (w), 1172 (w), 1106 (w), 1077 (w), 990 (w), 858 (w), 772 (w), 730 (w), 526(w).

#### 4.2.8. Synthesis of Pd(L<sub>4</sub>)<sub>2</sub>

In a flask, L<sub>4</sub> (0.053 g, 0.18 mmol) was dissolved in 10 mL ether and Pd(OAc)<sub>2</sub> (0.02 g, 0.09 mmol) was added to the flask. The mixture stirred at room temperature for 24 h. Then, the precipitate was collected by filtration and it was washed small amount of ether. Dark red supernatant from reaction and solution from precipitate wash was combined and left in a small glass vial at ambient temperature for crystallization. Due to low solubility of Pd(L<sub>4</sub>)<sub>2</sub> complex in deuterated solvents, a suitable  $^{13}\text{C}$  NMR spectrum was not obtained for this compound. Yield: 0.035 g, 56%. Mp: 186 °C.  $^1\text{H}$  NMR (Acetone- $d_6$ , 400 MHz):  $\delta$  7.88 (s,

2H), 7.58-7.55 (m, 4H), 7.50-7.48 (t, 2H), 7.00 (d, 2H,  $J = 8.0$  Hz), 6.71 (d, 2H,  $J = 8.0$  Hz), 6.46 (t, 2H), 3.47 (s, 6H). IR: 3441 (br.), 3000 (w), 2928 (w), 2820 (w), 1606 (m), 1577 (s), 1537 (m), 1460 (w), 1370 (w), 1327 (m), 1249 (s), 1203 (w), 1108 (w), 1076 (w), 969 (w), 857 (w), 784 (w), 736 (m), 646 (w), 464 (w).

### 4.3 Biological Assay

#### 4.3.1. Cell Lines and Cell Culture

Three human cell lines including MCF-7 (breast cancer), A549 (lung cancer), SKOV3 (ovarian cancer) were purchased from the National Cell Bank of Iran (NCBI, Pasteur Institute, Tehran, Iran). All cell lines were cultured in complete culture medium containing Roswell Park Memorial Institute (RPMI) 1640 medium (Biosera, UK), 10 % fetal bovine serum (FBS; Gibco, USA) and 1 % penicillin-streptomycin (Biosera, UK) and were incubated at 37 °C in a CO<sub>2</sub> incubator with 95% humidity. The cytotoxic effects of four Pd(II) complexes on these cell lines were assessed using the 3-(4,5-dimethylthiazolyl)-2,5-diphenyltetrazolium bromide (MTT) standard assay as described before [32,33]. Briefly, the cells were detached, counted and 10,000 cells were then seeded in 96-well microplate in 100 µl complete culture medium per well. The cells were incubated for 24 h and then treated with different concentrations of each compound in triplicate manner. The compounds were solved in DMSO (Sigma, Germany) and then diluted in culture medium to make different concentrations (1-100 µM). *cis*-platin with different concentrations was also used as positive control. Culture medium were added to three wells with and without cells considered as negative controls and blanks, respectively. The cells were incubated for 48 h at 37 °C in a humidified CO<sub>2</sub> incubator. The medium was completely removed and replaced by 100 µl RPMI containing MTT (0.5 mg/ml; Sigma, Germany) and incubated for more 3 h to formazan complexes were formed. The medium containing MTT was then completely poured out and 100 µl DMSO was added to each well to dissolve the formazan crystals and were incubated for 30 min. The absorbance of each well was read at 495 nm with a microplate ELISA reader. The data were analyzed and 50 % inhibitory concentration (IC<sub>50</sub>) for each compound were obtained by CurveExpert 4.1. Data are presented as mean ± SD. Each experiment was independently repeated three times.

### 4.3.2 Apoptosis Detection

The induction of apoptosis by Pd(L<sub>1</sub>)<sub>2</sub> on MCF-7 cell line was determined by BioLegend's Annexin V Apoptosis Detection Kit (Biolegend, USA) according to manufactured instruction. Briefly, the cells were treated with three different concentrations of Pd(L<sub>1</sub>)<sub>2</sub> including IC<sub>50</sub> concentration (2, 7 and 14 μM) for 48 h. The cells were then trypsinized and washed twice with cold BioLegend's Cell Staining Buffer and then re-suspended in Annexin V Binding Buffer. Two microliter FITC-conjugated Annexin V and then 2 μl of 7-AAD Viability Staining Solution were added to each tube containing 200 × 10<sup>3</sup> cells. The cells were gently vortexed and incubated for 15 min in the dark at room temperature and analyzed directly by four-color FACSCalibur flow cytometer (BD Biosciences, USA). At least 50,000 cells were acquired. The experiment was repeated two times and the data was analyzed by FlowJo software.

### 4.3.3 Interaction of Pd(L<sub>1</sub>)<sub>2</sub> with DNA

pET28a plasmid (5369 bp) in circular format was used to investigate the interaction of Pd(L<sub>1</sub>)<sub>2</sub> with DNA as previously described [34]. The same aliquots of circular form of pET28a plasmid (1250 ng) were prepared in a buffer containing Tris-HCl, pH = 8.5 (Roche, Germany) and were incubated with different concentrations of compound Pd(L<sub>1</sub>)<sub>2</sub> (100, 400 and 800 μM) at 37 °C for 48h. Untreated DNA and *cis*-platin treated DNA (in the same concentrations) were also included as negative and positive controls, respectively. Then, 8 μl of each sample was mixed with 3 μl KBC loading dye (Kawsar Biotec, Iran) and loaded onto 1% agarose gel (Invitrogen, USA) and electrophoresed for 90 min at 70 V in 0.5% TEA buffer. The gel was then visualized by a UV detector.

### 4.3.4 X-ray Crystal Structure Determination and Refinement

Crystals of Pd(L<sub>1</sub>)<sub>2</sub>, Pd(L<sub>2</sub>)<sub>2</sub> and Pd(L<sub>3</sub>)<sub>2</sub> were grown from the acetone solutions. The X-ray diffraction data were collected with an Oxford Sapphire CCD diffractometer using MoK $\alpha$  radiation  $\lambda = 0.71073 \text{ \AA}$ , at 293(2) K, by  $\omega$ -2 $\theta$  method. Structures were solved by the direct methods and refined with the full-matrix least-squares method on F<sup>2</sup> with the use of SHELX2014 program package [35]. Analytical absorption corrections were applied with CrysAlisPro 1.171.38.43 (Rigaku OD, 2015) [36] (Table 1). The absolute structure of Pd(L<sub>2</sub>)<sub>2</sub> was determined with the Flack method [37], with the Flack x being -0.04(2). Hydrogen atoms were located from the electron density maps and their positions were constrained in the

refinement with the appropriate AFIX commands as implemented in SHELX. The structural data have been deposited with Cambridge Crystallographic Data Centre, the CCDC numbers 1554780, 1554781 and 1554782 for Pd(L<sub>1</sub>)<sub>2</sub>, Pd(L<sub>2</sub>)<sub>2</sub> and Pd(L<sub>3</sub>)<sub>2</sub>, respectively.

### Acknowledgement

Funding for this work by the Institute for Advanced Studies in Basic Sciences (IASBS) Research Council and the Iran National Science Foundation (Grant no. 93039954) is acknowledged. Thanks are also due to Mr. Biglari, the operator of Bruker NMR spectroscopy instrument at IASBS, for taking time to record the NMR spectra of these compounds.

### References

1. Rosenberg, B., Vancamp, L., TROSKO, J. E., & MANSOUR, V. H. (1969). Platinum compounds: a new class of potent antitumour agents. *Nature*, 222(5191), 385-386.
2. Sherman, S. E., & Lippard, S. J. (1987). Structural aspects of platinum anticancer drug interactions with DNA. *Chemical Reviews*, 87(5), 1153-1181.
3. Reedijk, J. (2003). New clues for platinum antitumor chemistry: kinetically controlled metal binding to DNA. *Proceedings of the National Academy of Sciences*, 100(7), 3611-3616.
4. Lake, B. R., Bullough, E. K., Williams, T. J., Whitwood, A. C., Little, M. A., & Willans, C. E. (2012). Simple and versatile selective synthesis of neutral and cationic copper (I) N-heterocyclic carbene complexes using an electrochemical procedure. *Chemical Communications*, 48(40), 4887-4889.
5. Liu, W., & Gust, R. (2013). Metal N-heterocyclic carbene complexes as potential antitumor metallodrugs. *Chemical Society Reviews*, 42(2), 755-773.
6. Monteiro, D. C., Phillips, R. M., Crossley, B. D., Fielden, J., & Willans, C. E. (2012). Enhanced cytotoxicity of silver complexes bearing bidentate N-heterocyclic carbene ligands. *Dalton Transactions*, 41(13), 3720-3725.
7. Casini, A., & Messori, L. (2011). Molecular mechanisms and proposed targets for selected anticancer gold compounds. *Current topics in medicinal chemistry*, 11(21), 2647-2660.
8. Marta Nagy, E., Ronconi, L., Nardon, C., & Fregona, D. (2012). Noble metal-dithiocarbamates precious allies in the fight against cancer. *Mini reviews in medicinal chemistry*, 12(12), 1216-1229.
9. Zmejkovski, B. B., Savić, A., Poljarević, J., Pantelić, N., Arandžević, S., Radulović, S., & Sabo, T. J. (2014). Synthesis, characterization and in vitro antitumor activity of new palladium (II) complexes with (S, S)-R 2 edda-type esters. *Polyhedron*, 80, 106-111.

10. Barry, N. P., & Sadler, P. J. (2013). Exploration of the medical periodic table: towards new targets. *Chemical communications*, 49(45), 5106-5131.
11. Nagy, E. M., Nardon, C., Giovagnini, L., Marchio, L., Trevisan, A., & Fregona, D. (2011). Promising anticancer mono- and dinuclear ruthenium (III) dithiocarbamate complexes: systematic solution studies. *Dalton Transactions*, 40(44), 11885-11895.
12. Gennari, C., & Piarulli, U. (2003). Combinatorial libraries of chiral ligands for enantioselective catalysis. *Chemical reviews*, 103(8), 3071-3100.
13. Cole, B. M., Shimizu, K. D., Krueger, C. A., Harrity, J., Snapper, M. L., & Hoveyda, A. H. (1996). Discovery of Chiral Catalysts through Ligand Diversity: Ti-Catalyzed Enantioselective Addition of TMSCN to meso Epoxides. *Angewandte Chemie International Edition*, 35(15), 1668-1671.
14. Yoon, T. P., & Jacobsen, E. N. (2003). Privileged chiral catalysts. *Science*, 299(5613), 1691-1693.
15. Cozzi, P. G. (2004). Metal-Salen Schiff base complexes in catalysis: practical aspects. *Chemical Society Reviews*, 33(7), 410-421.
16. Hossain, S. M., Lakma, A., Pradhan, R. N., Chakraborty, A., Biswas, A., & Singh, A. K. (2015). Synthesis and characterization of a novel, ditopic, reversible and highly selective, "Turn-On" fluorescent chemosensor for Al<sup>3+</sup> ion. *RSC Advances*, 5(78), 63338-63344.
17. Das, M., Baig, F., & Sarkar, M. (2016). Photophysical properties of di-Schiff bases: evaluating the synergistic effect of non-covalent interactions and alkyl spacers in enhanced emissions of solids. *RSC Advances*, 6(63), 57780-57792.
18. Makio, H., Kashiwa, N., & Fujita, T. (2002). FI catalysts: a new family of high performance catalysts for olefin polymerization. *Advanced Synthesis & Catalysis*, 344(5), 477-493.
19. Pasatoiu, T. D., Sutter, J. P., Madalan, A. M., Fellah, F. Z. C., Duhayon, C., & Andruh, M. (2011). Preparation, crystal structures, and magnetic features for a series of dinuclear [Ni<sup>III</sup>Ln<sup>III</sup>] Schiff-Base complexes: evidence for slow relaxation of the magnetization for the Dy<sup>III</sup> derivative. *Inorganic chemistry*, 50(13), 5890-5898.
20. Hu, K. Q., Jiang, X., Wu, S. Q., Liu, C. M., Cui, A. L., & Kou, H. Z. (2015). Slow Magnetization Relaxation in Ni<sup>II</sup>Dy<sup>III</sup>Fe<sup>III</sup> Molecular Cycles. *Inorganic chemistry*, 54(4), 1206-1208.
21. Schaus, S. E., Brandes, B. D., Larrow, J. F., Tokunaga, M., Hansen, K. B., Gould, A. E., & Jacobsen, E. N. (2002). Highly selective hydrolytic kinetic resolution of terminal epoxides catalyzed by chiral (salen) Co<sup>III</sup> complexes. Practical synthesis of enantioenriched terminal epoxides and 1, 2-diols. *Journal of the American Chemical Society*, 124(7), 1307-1315.

22. da Silva, C. M., da Silva, D. L., Modolo, L. V., Alves, R. B., de Resende, M. A., Martins, C. V., & de Fátima, Â. (2011). Schiff bases: A short review of their antimicrobial activities. *Journal of Advanced research*, 2(1), 1-8.
23. Carreira, M., Calvo-Sanjuán, R., Sanaú, M., Zhao, X., Magliozzo, R. S., Marzo, I., & Contel, M. (2012). Cytotoxic hydrophilic iminophosphorane coordination compounds of d 8 metals. Studies of their interactions with DNA and HSA. *Journal of inorganic biochemistry*, 116, 204-214.
24. Carreira, M., Calvo-Sanjuán, R., Sanaú, M., Marzo, I., & Contel, M. (2012). Organometallic palladium complexes with a water-soluble iminophosphorane ligand as potential anticancer agents. *Organometallics*, 31(16), 5772-5781.
25. Lease, N., Vasilevski, V., Carreira, M., de Almeida, A., Sanaú, M., Hirva, P., & Contel, M. (2013). Potential anticancer heterometallic Fe–Au and Fe–Pd agents: initial mechanistic insights. *Journal of medicinal chemistry*, 56(14), 5806-5818.
26. Ma, D. L., He, H. Z., Leung, K. H., Chan, D. S. H., & Leung, C. H. (2013). Bioactive Luminescent Transition-Metal Complexes for Biomedical Applications. *Angewandte Chemie International Edition*, 52(30), 7666-7682.
27. Vicente, J., Abad, J. A., Clemente, R., López-Serrano, J., Ramírez de Arellano, M. C., Jones, P. G., & Bautista, D. (2003). Mercurated and palladated iminophosphoranes. Synthesis and reactivity. *Organometallics*, 22(21), 4248-4259.
28. Darabi, F., Hadadzadeh, H., Simpson, J., & Shahpiri, A. (2016). A water-soluble Pd (II) complex with a terpyridine ligand: experimental and molecular modeling studies of the interaction with DNA and BSA; and in vitro cytotoxicity investigations against five human cancer cell lines. *New Journal of Chemistry*, 40(11), 9081-9097.
29. Falvello, L. R., García, M. M., Lázaro, I., Navarro, R., & Urriolabeitia, E. P. (1999). Different coordinating behaviour of the imino-phosphoranes Ph<sub>3</sub>P $\xi$ NC(O)CH<sub>2</sub>Cl and Ph<sub>3</sub>P $\xi$ NC(O)-2-NC<sub>5</sub>H<sub>4</sub> towards M(II) complexes (M= Pd, Pt). *New Journal of Chemistry*, 23(2), 227-235.
30. Kapdi, A. R., & Fairlamb, I. J. (2014). Anti-cancer palladium complexes: a focus on PdX<sub>2</sub>L<sub>2</sub>, palladacycles and related complexes. *Chemical Society Reviews*, 43(13), 4751-4777.
31. Ulukaya, E., Ari, F., Dimas, K., Ikitimur, E. I., Guney, E., & Yilmaz, V. T. (2011). Anti-cancer activity of a novel palladium (II) complex on human breast cancer cells in vitro and in vivo. *European journal of medicinal chemistry*, 46(10), 4957-4963.
32. Fereidoonmezhad, M., Kaboudin, B., Mirzaee, T., Babadi Aghakhanpour, R., Golbon Haghighi, M., Faghieh, Z., & Shahsavari, H. R. (2017). Cyclometalated Platinum (II) Complexes Bearing Bidentate O, O'-Di (alkyl) dithiophosphate Ligands: Photoluminescence and Cytotoxic Properties. *Organometallics*, 36(9), 1707-1717.
33. Fereidoonmezhad, M., Niazi, M., Ahmadipour, Z., Mirzaee, T., Faghieh, Z., Faghieh, Z., & Shahsavari, H. R. (2017). Cyclometalated Platinum (II) Complexes Comprising

2-(Diphenylphosphino) pyridine and Various Thiolate Ligands: Synthesis, Spectroscopic Characterization, and Biological Activity. *European Journal of Inorganic Chemistry*, 2017(15), 2247-2254.

34. Fereidoonzehad, M., Niazi, M., Shahmohammadi Beni, M., Mohammadi, S., Faghieh, Z., Faghieh, Z., & Shahsavari, H. R. (2017). Synthesis, Biological Evaluation, and Molecular Docking Studies on the DNA Binding Interactions of Platinum (II) Rollover Complexes Containing Phosphorus Donor Ligands. *ChemMedChem*, 12(6), 456-465.

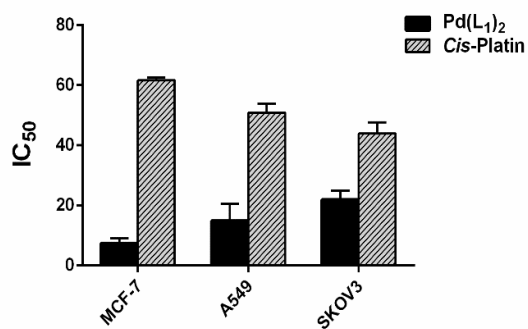
35. G. Sheldrick, A short history of *SHELX*. *Acta Cryst.*2008, **A64**, 112-122.

36. CrysAlisPro 1.171.38.43 package of programs, Rigaku OD, 2015.

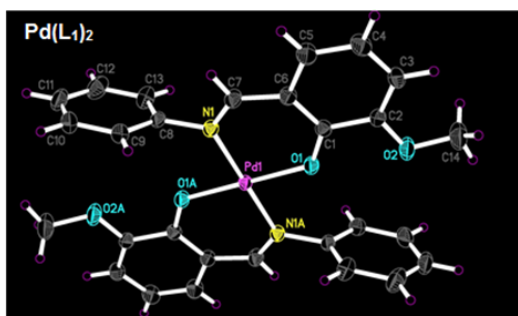
37. H.D. Flack, On enantiomorph-polarity estimation. *Acta Cryst.*, 1983, **A39**, 876-881.

**Palladium (II) complexes based on Schiff base ligands derived from *ortho*-vanillin; synthesis, characterization and cytotoxic studies**

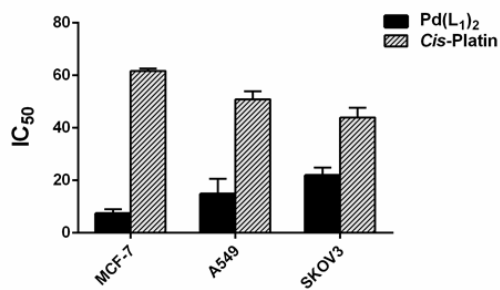
- \* Highly stable four coordinate palladium complexes
- \* Higher anti-proliferative activity on three cancerous cell lines than *cis*-platin



\*Higher anti-proliferative activity on three cancerous cell lines than *cis*-platin\*



\*Higher anti-proliferative activity on three cancerous cell lines than *cis*-platin\*



ACCEPTED MANUSCRIPT